



Electrical properties of Gd-modified PZT (MPB) ceramics

S C PANIGRAHI^{1,4}, PIYUSH R DAS^{2,*} and R PADHEE³

¹Department of Physics, Tihidi College, Tihidi 756 130, India

²Department of Physics, VSSUT, Burla, Sambalpur 768 018, India

³School of Physics, Sambalpur University, Burla, Sambalpur 768 019, India

⁴Department of Physics, Institute of Technical Education and Research, Siksha ‘O’ Anusandhan deemed to be University, Bhubaneswar 751 030, India

*Corresponding author. E-mail: prdas63@gmail.com

MS received 1 April 2020; revised 9 January 2021; accepted 12 March 2021

Abstract. The polycrystalline samples of gadolinium (Gd)-modified lead-zirconate-titanate ($\text{Pb}_{1-x}\text{Gd}_x(\text{Zr}_{0.52}\text{Ti}_{0.48})_{1-x/4}\text{O}_3$) ($x = 0, 0.07, 0.10$ and 0.12) (PGZT) ceramics near morphotropic phase boundary (MPB) were prepared by high-temperature solid-state reaction route. Electrical properties such as impedance (Z), modulus (M) and conductivity (σ) of the materials have been investigated within a wide range of temperature and frequency. Complex impedance spectroscopy (CIS) studies show that materials exhibit bulk (grain) resistive contributions, negative temperature coefficient of resistance (NTCR) and non-Debye-type dielectric relaxation. The nature of temperature and frequency dependence of conductivity follows Jonscher’s universal power law. $J-E$ characteristics reveal that the materials exhibit semiconducting behaviour and allow a very small leakage current to pass through them.

Keywords. Ceramics; solid-state reaction; morphotropic phase boundary; negative temperature coefficient of resistance; conductivity; complex impedance spectroscopy.

PACS Nos 77.80.-e; 84.37.+q; 72.80.Tm

1. Introduction

Lead zirconate titanate (commonly known as PZT) ceramics, a binary solid solution of ferroelectric PbTiO_3 (PT with T_c (Curie temperature) = 490°C) and antiferroelectric PbZrO_3 (PZ with $T_c = 230^\circ\text{C}$) with different Zr/Ti ratios belong to the perovskite family of a general formula ABO_3 in which site A is occupied by Pb^{2+} ions and site B by Zr^{4+} and/or Ti^{4+} ions [1]. As the properties of PZT ceramics are very much sensitive near the morphotropic phase boundary (MPB) separating the ferroelectric tetragonal (FT) and ferroelectric rhombohedral (FR) phases due to spontaneous polarisation in different directions over a wide range of temperature in the phase diagram [2,3], PZT materials can be used in various device applications such as FRAM, MEMS, charge storage, transducer, oscillators, pyroelectric devices, actuators and sensors [4–8].

To enhance the electrical and electromechanical properties of the materials greatly, various kinds of modifications can be made by suitable substitutions at A(Pb) or B(Zr/Ti) sites of PZT ceramics [9–13]. Out of them, the higher valence cations like La^{3+} , Gd^{3+} , Sm^{3+} , Dy^{3+} ,

Th^{4+} , Nb^{5+} etc. as donor (soft) dopant produce Pb-vacancies to maintain electrical neutrality and domain wall mobility that results high relative permittivity with high electromechanical properties [14–16].

Detailed literature survey of pure and modified PZT ceramics indicates that most of the reported works in this field are confined to La-modified PZT [17–20] ceramics. However, the rare-earth element gadolinium (Gd^{3+}) also satisfies the basic requirements for its substitution in PZT to avail the required ferroelectric properties for suitable device applications [21–24]. It is found that Gd-modified PZT (named PGZT) ceramics with Zr/Ti ratio 52/48 exhibits high relative permittivity and piezoelectric coefficients with low tangent loss [25]. Again, no work on PGZT very close to MPB (Zr/Ti ratio such as 52:48) has been done on its impedance and modulus analysis.

Complex impedance spectroscopy (CIS) is a non-destructive method [26] to study the microstructural and electrical properties of polycrystalline oxides. This can correlate the structural and electrical characteristics of polycrystalline oxides in a wide range of frequencies and temperature. Therefore, in this paper we have

synthesised PGZT materials by high-temperature solid-state reaction method and report the effect of Gd on electrical properties such as impedance and modulus properties of MPB-PZT (52:48: x) using CIS technique with conductivity as a function of temperature and/or frequency.

2. Experimental

The polycrystalline samples of Gd-modified lead zirconate titanate with a general formula $\text{Pb}_{1-x}\text{Gd}_x(\text{Zr}_{0.52}\text{Ti}_{0.48})_{1-x/4}\text{O}_3$ (PGZT) ($x = 0, 0.07, 0.10, 0.12$) were prepared by a high-temperature solid-state reaction technique [27] using high-purity ($\geq 99.9\%$) ingredients: PbO, TiO_2 and Gd_2O_3 (M/s LOBA Chemie Pvt. Ltd., India), ZrO_2 (M/s Himedia Chemie Pvt. Ltd., India). Two mole% of excess PbO was taken to compensate for Pb loss during high-temperature calcinations and sintering. The stoichiometric amounts of the ingredient oxide powders were mixed thoroughly; first in an air atmosphere for 1 h and in wet medium (i.e. methanol) for 1 h in agate mortar. The calcination temperature for the homogeneous mixture was decided and optimised (1100°C) on the basis of repeated firing/mixing for 4 h in high-purity (99.9%) alumina crucible.

A preliminary X-ray diffraction (XRD) pattern (on final calcinated powders) was obtained at room temperature using X-ray powder diffractometer (XPRT-PRO). The calcinated powders were then cold pressed into cylindrical pellets of 10 mm diameter and 1–2 mm of thickness under a uniaxial pressure of $4 \times 10^6 \text{ N/m}^2$ using a hydraulic press. A small amount polyvinyl alcohol (PVA) was used as a binder to prepare the pellet which was burnt out due to high-temperature sintering. The pellets were sintered at an optimised temperature of 1150°C for 4 h in air atmosphere. In order to prevent PbO loss during high-temperature sintering and to maintain the desired stoichiometry, an equilibrium PbO vapour pressure was developed with PbZrO_3 as the setter by placing pellets in a covered alumina crucible. The microstructure and texture of the gold-coated pellets were recorded using a JEOL JSM-5800 scanning electron microscope (SEM) at different magnifications.

The sintered pellets were coated with high-quality silver paste and dried at 160°C for 6 h before taking electrical measurements. The dielectric (capacitance and dissipative factor) and electrical (impedance, phase angle, inductance, modulus, conductivity etc.) parameters of the sintered pellet samples were measured as a function of frequency (from 1 kHz to 1 MHz) at different temperatures ($25\text{--}500^\circ\text{C}$) using a computer-controlled phase-sensitive meter (PSM LCR 4NL: 1735, UK) with a laboratory-designed and fabricated sample holder and

small vertical pit furnace. A chromel-alumel thermocouple and digital milli-voltmeter (KUSUM MECO108) were used to record the temperature.

The temperature dependence of the $I\text{--}V$ characteristics of the sintered pellet samples were obtained in a wide range of voltage (0–100 V) and temperature ($25\text{--}500^\circ\text{C}$) using programmable electrometer (model 6517B; Keithley), sample holder and pit furnace.

3. Results and discussions

We have already reported the formation of single-phase PGZT compounds with rhombohedral unit cell using XRD and distribution of grains in scanning electron micrographs [25]. From the structural analysis, it is suggested that there is no change in basic rhombohedral crystal structure of PGZT $x/52/48$ ceramics on Gd substitution within the studied composition range ($x = 0, 0.07, 0.10, 0.12$). The volume of the unit cell and cell parameter were found to be decreasing for $x \leq 0.10$ and increasing for $x > 0.10$ on substituting Gd at Pb site of PGZT $x/52/48$ ceramics. The variation of volume of the unit cell and cell parameter of PGZT $x/52/48$ ceramics suggests that Gd^{3+} ion enters at A sites up to 10% and then enters B-sites for the higher concentration of Gd to compensate the excess positive charge by the creation of vacancies at favourable respective sites of A/B [25]. The average crystallite size of the PGZT $x/52/48$ samples is found to be in the range of 22–11 nm [25]. In SEM it was found that the grains of different sizes are uniformly distributed over the entire surface of the samples. Most of the grains were found to be more or less spherical in nature and in some cases rectangular in shape with the average grain size in the range of 1–5 μm [25].

In the studied PGZT materials, the composition of Zr/Ti ratio is chosen as 52:48 near MPB to support the change in intrinsic properties of PZT ceramics for a wide range of temperature as MPB line is nearly vertical in the phase diagram. Again, Gd^{3+} substitution at Pb^{2+} site act as higher valent dopants and render the PZT ‘soft’ which is characterised by higher permittivity, higher piezoelectric coefficients, higher order resistivity and low tangent loss. Dielectric and piezoelectric properties of the studied materials are reported in [25]. The increase of Gd^{3+} substitution disrupts the ferroelectric long-range ordering, leading to an increase in compositional disorder, and as a result, dielectric and ferroelectric characteristics of the samples change significantly. The substitution of Gd^{3+} on Pb^{2+} site creates some oxygen vacancies and/or lattice distortion in the studied materials. Due to the high-temperature sintering process and volatile nature of Pb, space charges and

oxygen vacancies are created and as a result, the impact of ferroelectric domain wall pinning on the modification of physical properties of the materials may likely to be noticed. Again, on addition of Gd^{3+} , Pb vacancies make the transfer of atoms easier than in a perfect lattice, and thus domain wall motions can be caused by smaller electric field/mechanical stress. Hence, with increasing concentration of Gd (x) in PGZT $x/52/48$ ceramics, polarisation increases.

3.1 Impedance and modulus spectroscopy

Microstructural and electrical properties of the polycrystalline PGZT ceramics in a wide range of frequency and temperature were analysed using complex impedance spectroscopy (CIS) technique [26]. It is a simple non-destructive technique and is used to separate the contributions of grain, grain boundary and interface properties of ceramics in complex impedance plane and other related electrical parameters with different equivalent circuits. It analyses the AC response of the system to a sinusoidal perturbation in the measurement of real and imaginary components of the complex electric parameters. For this analysis, the standard basic equations of impedance and electric modulus are as follows:

$$\text{Complex impedance: } Z^*(\omega) = Z' - jZ'' = R_s - \frac{j}{\omega C_s}$$

$$\text{Complex permittivity: } \varepsilon^*(\omega) = \varepsilon' - j\varepsilon''$$

$$\begin{aligned} \text{Complex modulus: } M^*(\omega) &= \frac{1}{\varepsilon^*(\omega)} = M' + jM'' \\ &= j\omega C_0 Z^* \end{aligned}$$

$$\begin{aligned} \text{Complex admittance: } Y^*(\omega) &= Y' + jY'' = j\omega C_0 \varepsilon^* \\ &= \frac{1}{R_p} + j\omega C_p \end{aligned}$$

$$\text{Loss tangent: } \tan \delta = \frac{\varepsilon''}{\varepsilon'}$$

where $j = \sqrt{-1}$, $\omega = 2\pi f$ is the angular frequency, C_0 is the geometrical capacitance, (Z', M', ε') and $(Z'', M'', \varepsilon'')$ are the real and imaginary components of impedance, modulus and permittivity respectively. The subscripts p and s refer to parallel and series circuit components respectively. In this technique, the interpretation of experimental data is done by an equivalent circuit model representing the realistic material properties and it is obtained by a series combination of grain and grain boundary, each represented by a parallel RC element.

The impedance data of the materials are generally plotted in complex plane plots (i.e., Z'' vs. Z') called Nyquist plot (named after Harry Nyquist, a former Engineer at Bell Laboratories, USA) with each point

corresponding to a different frequency. In Cartesian coordinates, the real part (Z') of impedance (system function) is plotted on the abscissa and imaginary part (Z'') is plotted on the ordinate. It is a parametric plot of a frequency response used in impedance analysis for assessing the stability of materials. This spectrum is characterised by (i) the appearance of semicircular arcs with a tendency to form a second semicircle which corresponds to bulk (grain) along with the grain boundary property of materials and (ii) depressed semicircle representing non-Debye-type of relaxation. Figures 1a–1d show the temperature dependence of complex impedance spectra (Nyquist plot) of PGZT $x/52/48$ ($x = 0, 0.07, 0.10, 0.12$) over a wide range of frequency (from 1 kHz to 1 MHz). This spectrum is characterised by the appearance of semicircular arc which is temperature dependent. In the studied materials, the nature of the plots suggests that (i) depressed semicircles indicate the presence of non-Debye-type of relaxation and (ii) the presence of single semicircle is due to the bulk property of materials [28]. Figures 1a–1d (inset) compare the experimental and model-fitted impedance (calculated using the software ZSIMPWIN version 2.0) values. An excellent agreement between the experimental and calculated values of both real and imaginary parts of impedance was found. Calculated values of bulk resistance (R_b) and bulk capacitance (C_b) at different temperatures from fitted curves are compared in table 1. The value of R_b initially increases up to $x \leq 0.10$ and then decreases for PGZT $x/52/48$ ceramics. This result can be correlated with the crystallite size and shape of the grain of the studied samples, which was reported in the previous paper [25]. In the studied samples, it was observed that (i) the average particle size first decreases up to $x \leq 0.10$ and then increases, (ii) the shapes of the grains are more or less spherical for $x \leq 0.10$ and rectangular for $x > 0.10$. Hence, the resistance/resistivity of the studied samples increases with decreasing crystallite size and also depends upon the shape of grains in its microstructure of the studied samples. The decreasing trend in the value of R_b and C_b with rise in temperature clearly indicates the existence of negative temperature coefficient of resistance (NTCR) in the materials as in semiconductors [29]. On substitution of Gd, radius of the semicircle increases largely up to $x = 0.07$ and then decreases slowly up to $x = 0.12$ which gives an indication of increasing resistance of the PGZTs with respect to PZT material. The above observed result is consistent with the reported soft-PZT compounds [9,30].

Figures 2a–2d show the variation of real part of impedance (Z') as a function of frequency at selected temperatures for the samples of PGZT $x/48/52$ ($x = 0, 0.07, 0.10$ and 0.12). There is a decrease in the values of Z' with rising temperature and frequency contributes

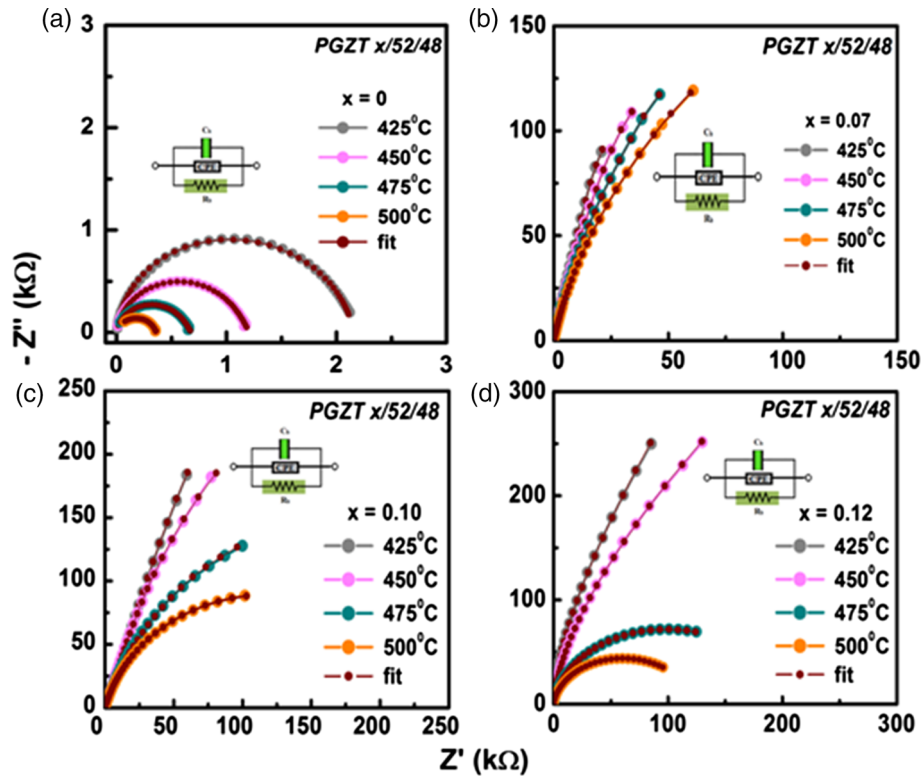


Figure 1. Variation of Z'' with Z' of $\text{Pb}_{1-x}\text{Gd}_x(\text{Zr}_{0.52}\text{Ti}_{0.48})_{1-x/4}\text{O}_3$ (PGZT) ceramics when (a) $x = 0$, (b) $x = 0.07$, (c) $x = 0.10$, (d) $x = 0.12$ at different temperatures.

Table 1. Comparison of bulk resistance and capacitance at different temperatures of PGZT ceramics ($x = 0, 0.07, 0.10, 0.12$).

Composition PGZT $x/52/48$	Temp. ($^{\circ}\text{C}$)	R_b (Ω)	C_b (F)
$x = 0.00$	425	2.1×10^3	2.4×10^{-10}
	450	1.2×10^3	2.1×10^{-10}
	475	6.7×10^2	1.3×10^{-10}
	500	3.6×10^2	7.4×10^{-11}
$x = 0.07$	425	7.8×10^6	1.0×10^{-9}
	450	3.7×10^6	7.7×10^{-10}
	475	1.9×10^6	5.1×10^{-10}
	500	6.5×10^5	4.6×10^{-10}
$x = 0.10$	425	6.4×10^6	2.3×10^{-10}
	450	3.9×10^6	1.1×10^{-10}
	475	4.8×10^5	8.2×10^{-11}
	500	2.4×10^5	6.1×10^{-11}
$x = 0.12$	425	1.3×10^6	1.4×10^{-9}
	450	4.1×10^5	4.3×10^{-10}
	475	2.4×10^5	2.5×10^{-10}
	500	1.3×10^5	2.2×10^{-10}

to increase in AC electrical conductivity in the materials [31]. At all the temperatures, the value of Z' decreases with increasing frequency indicating the possibility of

increase in the AC conductivity. At lower frequencies, the decrease in the magnitude of Z' with rise in the temperature reveals their NTCR behaviour. The behaviour of Z' -plots changes drastically at high frequencies and shows a complete merger beyond a certain frequency. The merger Z' at high frequencies, may occur due to the release of space charge and a consequent lowering of the barrier properties in the materials [23].

Figures 3a–3d show the variation of imaginary part of impedance (Z'') as a function of frequency (loss spectrum) at selected temperatures for the samples of PGZT $x/52/48$ ($x = 0, 0.07, 0.10$ and 0.12). These plots provide an insight into the electrical processes having the largest resistances and suitable for evaluation of the relaxation frequency of the most resistive component. This loss spectrum is characterised by low-frequency dispersion and merger at higher frequencies which is due to the presence of space charge polarisation at lower frequency and its elimination at higher frequency. At low temperatures, the relaxation process may be attributed to the presence of mobile species (electrons) and/or immobile species, while at higher temperatures the same may occur due to vacancies and/or defects [31,32]. At high temperatures, the appearance of peak is an indication of the electrical relaxation in the materials. Asymmetry peak pattern broadening indicates the deviation from

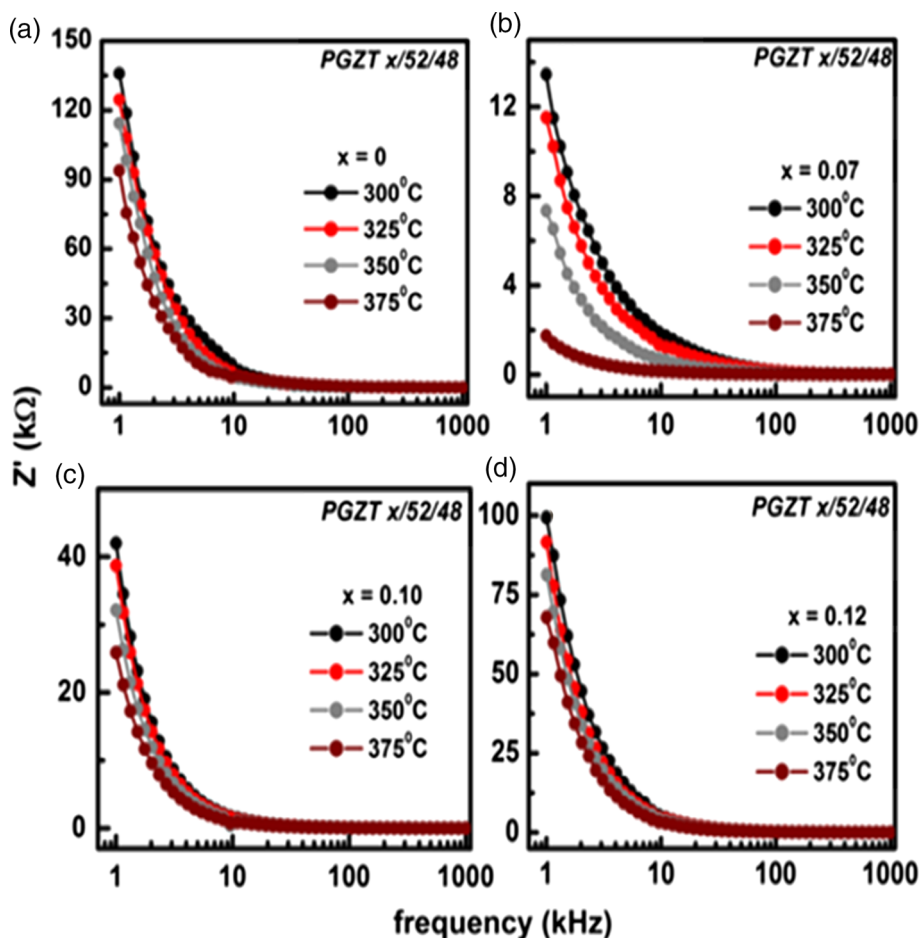


Figure 2. Variation of Z' with frequency of PGZT ceramics when (a) $x = 0$, (b) $x = 0.07$, (c) $x = 0.10$, (d) $x = 0.12$ at different temperatures.

the ideal Debye behaviour. The frequency at which the value of Z'' attains a maxima Z''_{max} is called relaxation frequency (ω_{max}) of the materials. ω_{max} shifts towards higher frequency region with increasing temperature. The broadening of peaks and decreasing value of Z''_{max} with rise in temperature suggests the occurrence of temperature dependence of relaxation phenomenon. On substituting Gd, (i) the relaxation process is shifted to low-frequency range (below 1 kHz) which was not observed due to our experimental limitations and (ii) at higher temperatures, absence of peaks suggests the significant decrease of loss tangent in PGZT samples. Hence, relaxation property is the function of not only temperature but also the concentration of Gd.

The electrical response of the materials can be analysed through complex electric modulus ($M^* = 1/\epsilon^*(\omega) = M' + jM'' = j\omega C_0 Z^*$), where M' and M'' are usually known as real and imaginary parts of the modulus. This formalism corresponds to the relaxation of the electric field in the material by keeping electric displacement constant and gives insight into the bulk

response using its capacitive nature. Figures 4a–4d show the variation of the imaginary part of the modulus (M'') with respect to frequency at selected temperatures for the samples of PGZT $x/52/48$ ($x = 0, 0.07, 0.10$ and 0.12). It exhibits asymmetric peak (or its tendency) in the low- as well as high-frequency region in the studied frequency range. The existence of low-frequency peak suggests that ion can move over long distances, whereas high-frequency peak suggests the restriction of ions in their potential well. These two peaks (double relaxation) indicate the transition from long-range mobility to short-range mobility on increasing the frequency [33]. The temperature dependence of asymmetric broadening of the peak is observed which confirms the spread of relaxation with different time constants, and hence the relaxation in the material is considered to be non-Debye-type [34]. The plot also shows that peak shifts towards higher frequency side with rise in temperature and this behaviour confirms that dielectric relaxation in the material is due to a thermally activated process in which hopping of charge carriers with small polarons are dom-

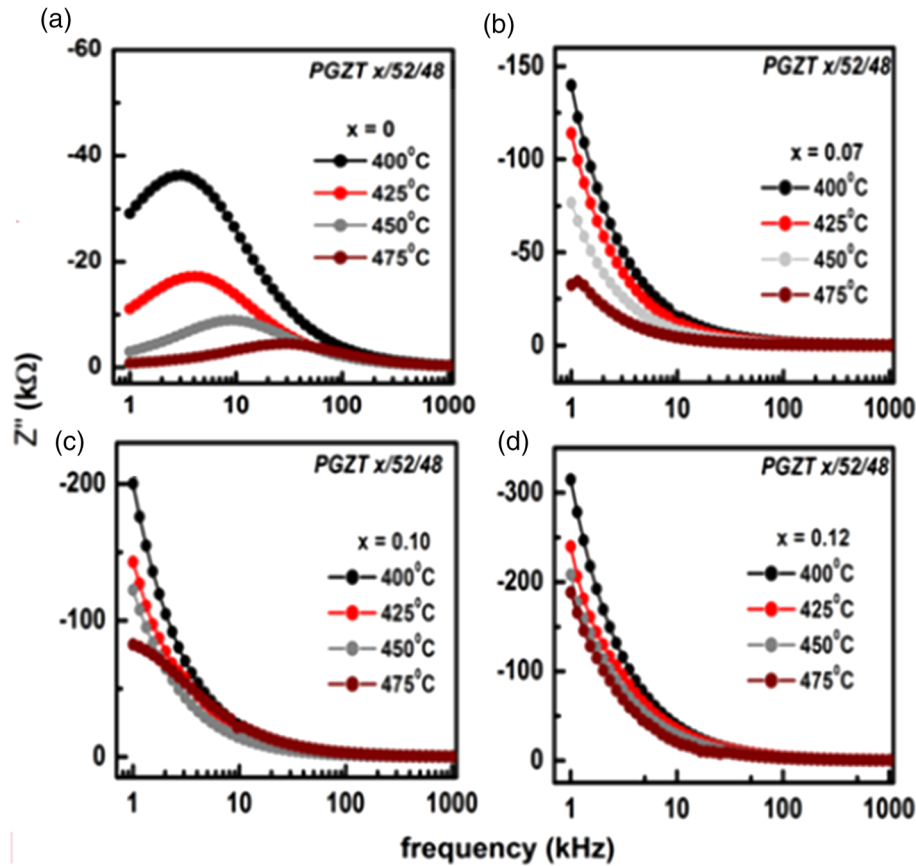


Figure 3. Variation of Z'' with frequency of PGZT ceramics when (a) $x = 0$, (b) $x = 0.07$, (c) $x = 0.10$, (d) $x = 0.12$ at different temperatures.

inated intrinsically for all the compounds. The nature of peaks and the value of M'' corresponding to peaks (M''_{\max}) depends upon Gd concentration in PGZTs. It is observed that there is double relaxation for $x = 0.07$ and 0.10 of PGZT and value of M''_{\max} decreases upto 7% and then increases up to 12% of Gd in PGZT compounds.

Figures 5a–5d show the variation of M' of PGZT $x/52/48$ ($x = 0, 0.07, 0.10$ and 0.12) compounds as a function of frequency at selected temperatures. It shows a very low value (approximately zero) of M' in the low-frequency region. A continuous dispersion on increasing frequency with a tendency to saturate at maximum value signifies short-range mobility of charge carriers in conduction mechanism of the studied materials. This may be contributed to a lack of restoring force governing the mobility of the charge carriers under the action of induced electric field [35]. There is a temperature-dependent relaxation process as the value of M' increases with the increase in temperature. The plateau region or its tendency observed at high frequency region signifies the frequency invariant (DC conductivity) electrical properties of the materials. It is also observed that the value of M' increases with the increase in Gd concentration of PGZT ceramics.

3.2 AC Conductivity

It is difficult to describe the motion of charge carriers in ceramic materials because various complex dynamic processes are involved. However, conductivity can be described as an acceptable way for the electrical properties of the studied materials. It is well known that PZT ceramics possesses p-type conductivity (hole-type conduction), caused by Pb loss due to high volatility of PbO during the sintering process [36,37]. Here, in soft-doped ceramics (PGZT), Pb^{2+} is replaced by substitution of Gd^{3+} and this substituted ion acts as a centre of positive electric charge similar to donor impurities in semiconductors. Figures 6a–6d show the plot of σ_{AC} of PGZT $x/52/48$ for different concentrations of Gd ($x = 0, 0.07, 0.10$ and 0.12) against the inverse absolute temperature ($10^3/T$) at different frequencies. The nature of variation of curves over a wide temperature range supports the temperature dependence of transport properties of the materials obeying Arrhenius equation: $\sigma = \sigma_0 e^{E_a/K_B T}$ [30], where σ_0 , E_a and K_B are pre-exponential factor, activation energy and Boltzmann constant respectively. An increase in conductivity around T_c signifies the increase of polarisability of the

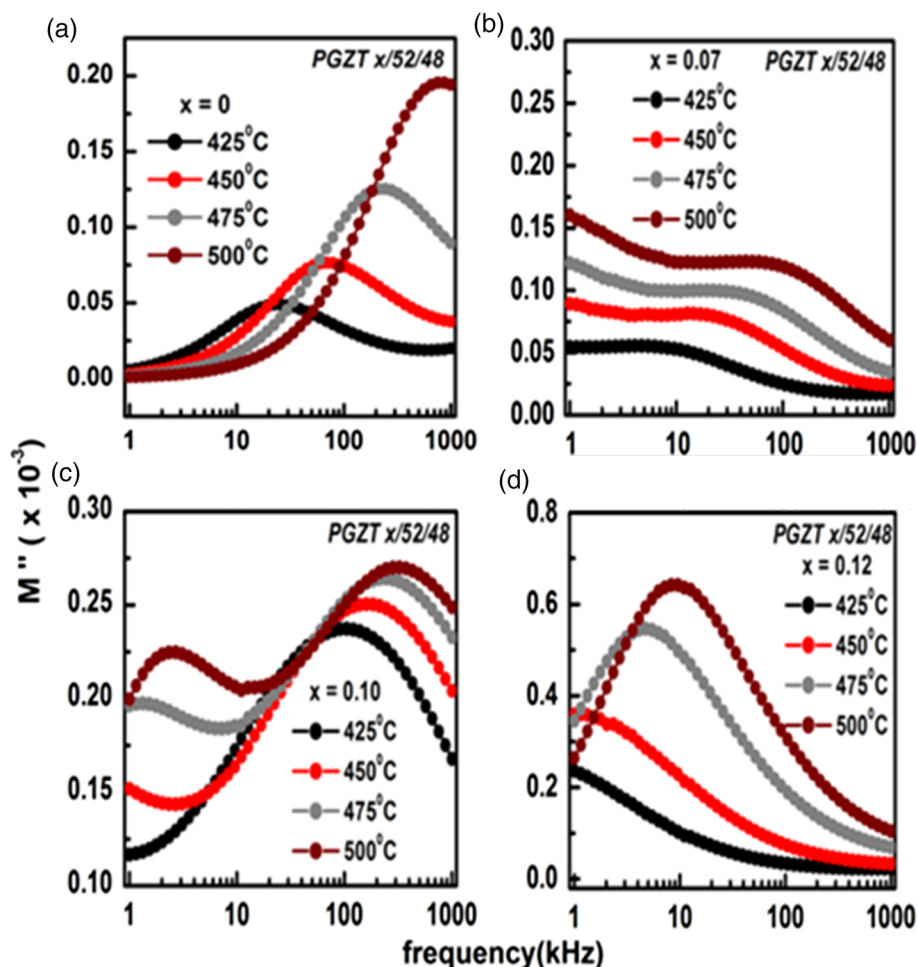


Figure 4. Variation of M'' with frequency of PGZT ceramics when (a) $x = 0$, (b) $x = 0.07$, (c) $x = 0.10$, (d) $x = 0.12$ at different temperatures.

material. Above T_c the conductivity data tend to fall and then increase, which is a typical behaviour of the DC component of conductivity [15], and significant increase of $\tan \delta$. The estimated values of E_a (from the slope of Arrhenius plots) are 0.29 eV, 0.34 eV, 0.36 eV, 0.38 eV at 100 kHz in the ferroelectric (FE) phase (245–340°C) and 0.31 eV, 0.39 eV, 0.40 eV, 0.42 eV in paraelectric (PE) phase (440–482°C) for $x = 0, 0.07, 0.10$ and 0.12 respectively. The values of activation energy in the PE phase are comparatively greater than that in the FE phase. Again, with increasing concentration of Gd, the activation energy increases leading to a decrease of p-type conductivity in the studied PGZT $x/52/48$ samples.

The frequency dependence of AC conductivity was analysed to study the electrical properties of the materials. The conduction mechanism of these materials is in accordance with Jonscher's Universal power law [24,38], $\sigma_{AC} = \sigma_{DC} + A\omega^n$, where A is a thermally activated constant which determines the strength of polarisability and n determines the degree of interac-

tion between the mobile ions and lattices. The value of $n < 1$ signifies the translational motion with sudden hopping whereas $n > 1$ involves the localised hopping without the species leaving the local surroundings [39]. The frequency at which change of slope of curve occurs is known as hopping frequency (ω_p). According to Jonscher [38], the origin of the frequency dependence of conductivity lies in the relaxation phenomena arising due to mobile charge carriers. When a mobile charge carrier hops to a new site from its original position, it remains in a state of displacement between two potential energy minima. Figure 7 shows the variation of σ_{AC} with frequency (with non-linear fitting) at 300°C of PGZT $x/52/48$ for $x = 0, 0.07, 0.10$ and 0.12. The high-frequency dispersion has been attributed to the AC conductivity whereas the frequency-independent plateau region corresponds to the DC conductivity. The pattern of conductivity spectrum shows some typical features such as (i) dispersion throughout the frequency range of investigation and (ii) low-frequency plateau and high-frequency dispersion. The characteristics of low-

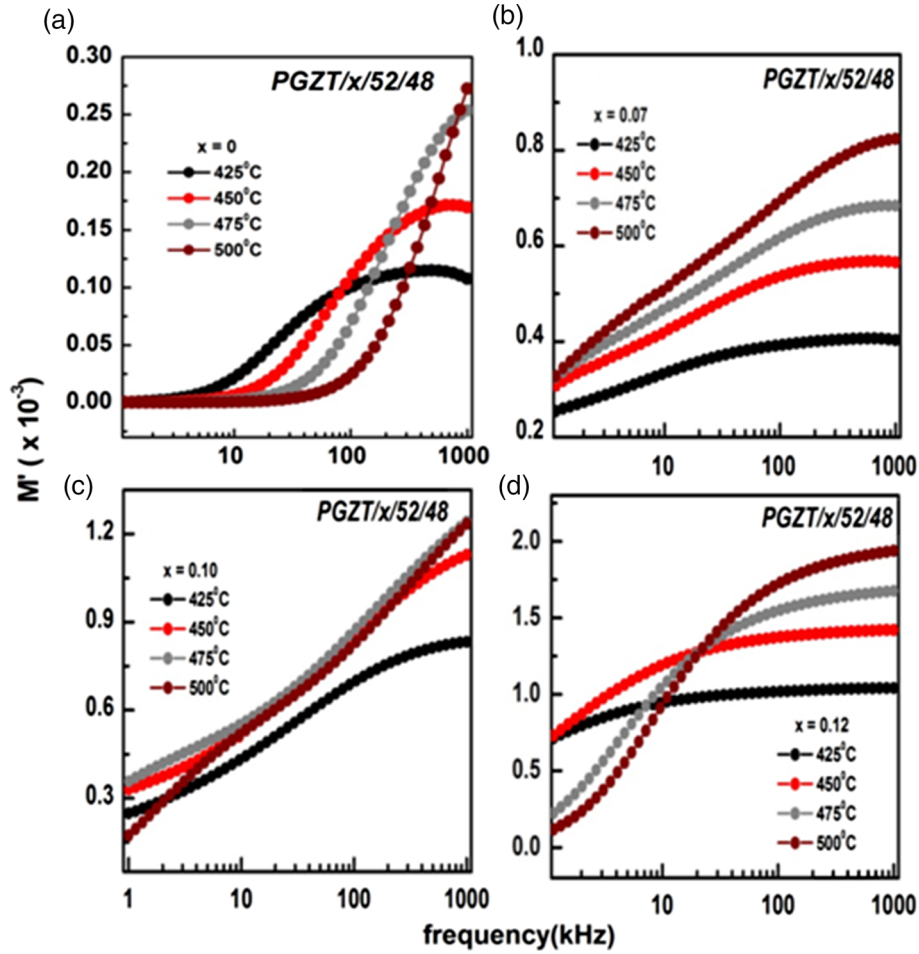


Figure 5. Variation of M' with frequency of PGZT ceramics when (a) $x = 0$, (b) $x = 0.07$, (c) $x = 0.10$, (d) $x = 0.12$ at different temperatures.

frequency plateau in the materials is more pronounced at lower concentration of Gd in PGZT $x/52/48$ ceramics. The studied materials obey universal power law which is confirmed by fit of the above equation to the experimental data (figure 7), where solid line corresponds to fitted curve and symbols represent the experimental data. These phenomena are consistent with other related PZT compounds [40].

To study the frequency dependence of the AC conductivity, we have followed Jonscher's universal power law [16,38] to provide the nature of charge carriers in conduction mechanism of the studied materials such as

$$\sigma_{\text{total}}(T, \omega) = \sigma_{\text{DC}}(T) + \sigma_{\text{AC}}(T, \omega);$$

$$\sigma_{\text{AC}}(T, \omega) = A(T) \omega^n,$$

where $\sigma_{\text{DC}}(T)$ is the frequency independent term which gives DC conductivity and $\sigma_{\text{AC}}(T, \omega)$ is the dispersive component of AC conductivity. The exponent (n) represents degree of interaction of mobile ions with lattices and the thermally activated constant (A) determines

the strength of polarisability. These fitting parameters (A and n) are obtained from the non-linear fitting of AC conductivity spectrum of the studied materials. For all the studied materials, the smaller value of n (< 1) suggests that the motion of hopping charge carriers is translational. Figure 8 shows the variation of fitting parameters A and n as a function of temperature of $\text{Pb}_{1-x}\text{Gd}_x(\text{Zr}_{52}\text{Ti}_{48})_{1-x/4}\text{O}_3$ ($x = 0, 0.07, 0.10, 0.12$) ceramics. For all the samples, it is observed that the value of n initially decreases with rise in temperature and then increases after T_c . The minimum value of n at T_c suggests a strong interaction between mobile ions with the lattice around them, which is due to diminishing restoring force for weakening the transverse optical mode (soft mode). Hence, the enhancement of conductivity near T_c is accounted for the coupling of charge carriers with this soft mode [16,38]. The variation of A with temperature is in reverse manner as n varies with temperature and the maximum value of A at T_c suggests high polarisability.

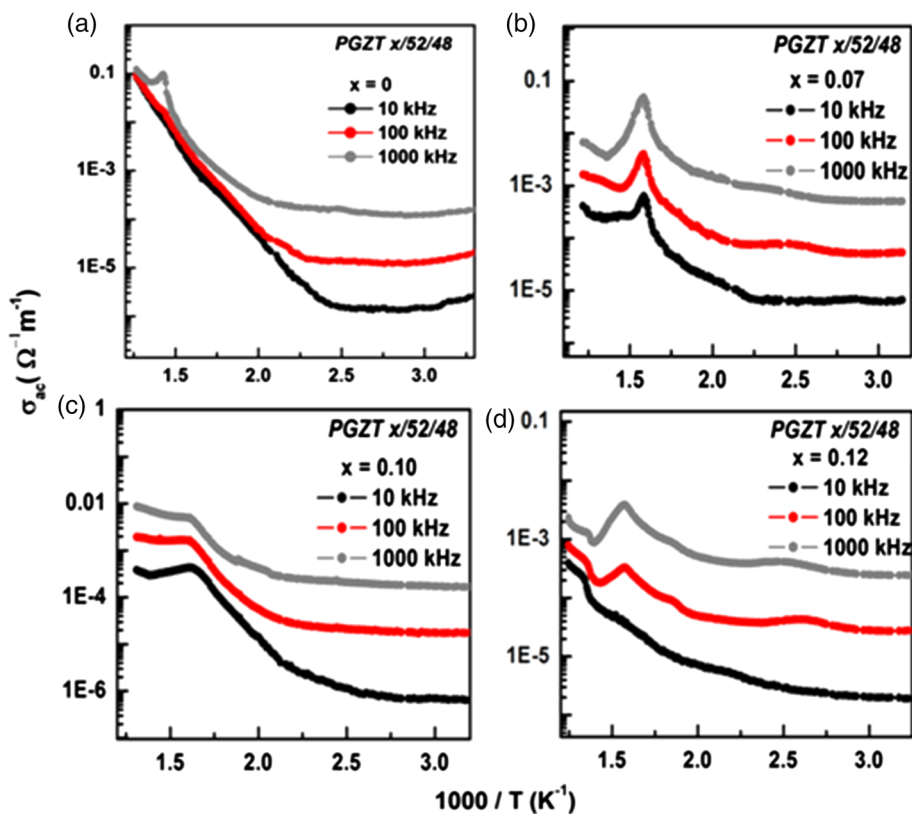


Figure 6. Variation of σ_{AC} with $10^3/T$ of PGZT ceramics when (a) $x = 0$, (b) $x = 0.07$, (c) $x = 0.10$, (d) $x = 0.12$ at different frequencies.

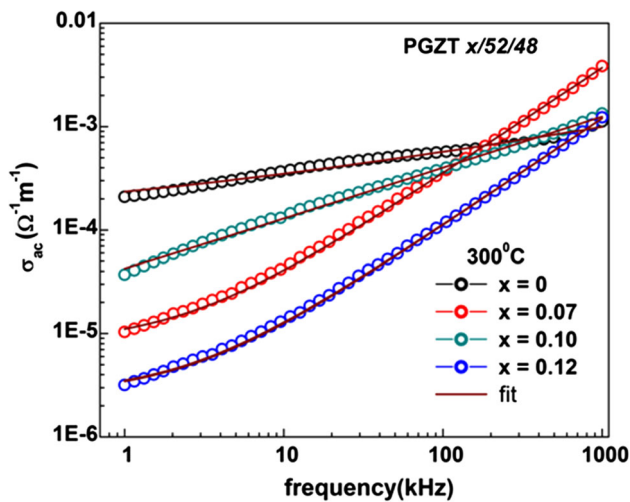


Figure 7. Variation of σ_{AC} with frequency of PGZT ceramics ($x = 0, .07, 0.10, 0.12$) at 300°C .

3.3 J – E characteristics

PGZT ceramics are widely used in electronic circuits because of their high value of resistivity and small temperature coefficient of resistance. It is useful to have a resistor that offers low resistance at high voltage and

high resistance at low voltage as the case in current–voltage (I – V) characteristics/current density–electric field (J – E) study. J – E characteristics study of ferroelectric ceramics is a useful technique to understand the conduction mechanism in a sample. Figures 9a–9d show the variation of current density (J) with applied DC electric field (E) of PGZT $x/52/48$ for $x = 0, 0.07, 0.10$ and 0.12 at some selected temperatures. For all the samples, it is observed that (i) the current density increases with rise in the temperature, thus indicating their NTCR behaviour and (ii) the value of current density increases rapidly on increasing the electric field, thus indicating their semiconducting nature [41,42]. The curves also reveal that the materials allow a very small leakage current to pass through them. The slope of these characteristic curves gives DC conductivity of the corresponding samples. The increase in slope of the characteristic curves with rise in the temperature suggests an increase in DC conductivity of the materials, thus confirming their NTCR behaviour. The curves also predict that, the studied materials follow Ohmic behaviour ($J \propto E^\beta; \beta \sim 1$) in the low electric field region and obey Child’s law ($J \propto E^\beta; \beta > 1$) in the high electric field region. Hence in high-electric field and high-temperature region, the conduction mecha-

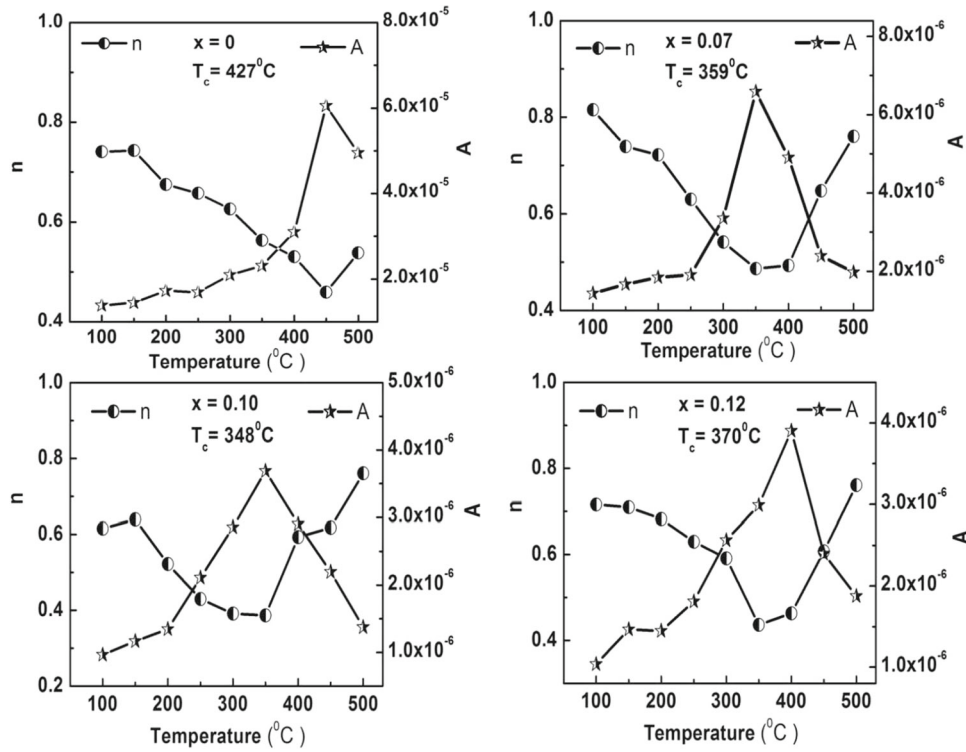


Figure 8. Variation of fitting parameters A and n as a function of temperature of PGZT ceramics ($x = 0, 0.07, 0.10, 0.12$).

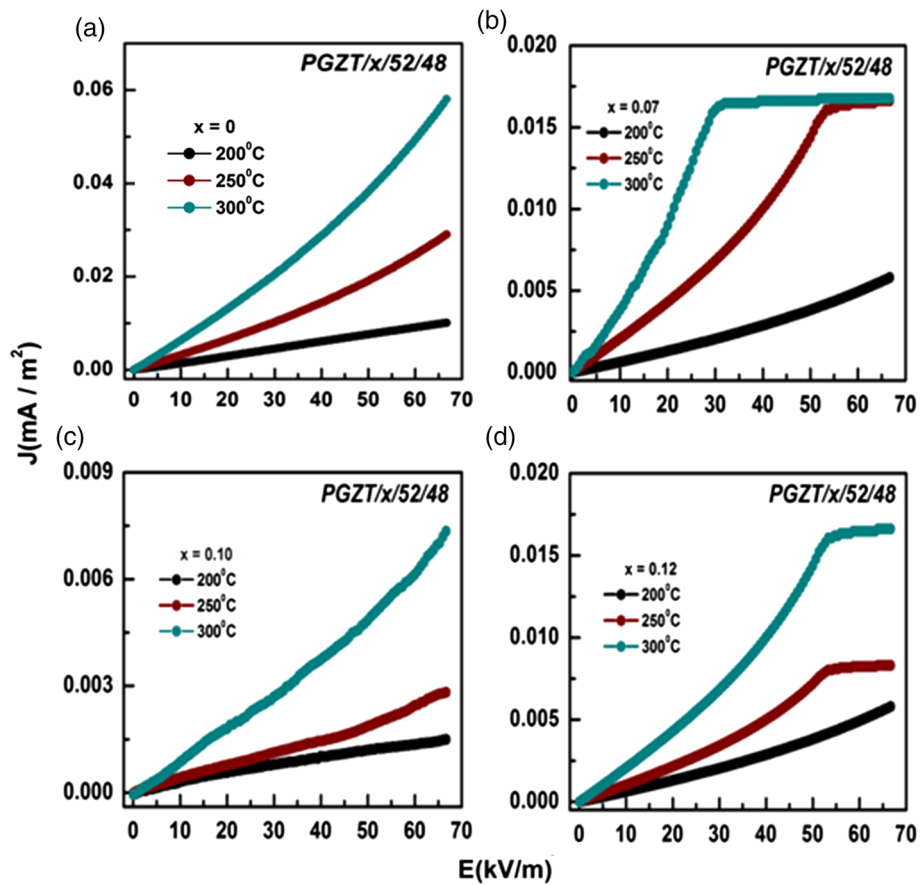


Figure 9. Temperature variation of $J-E$ characteristics of PGZT ceramics ($x = 0, 0.07, 0.10, 0.12$).

nism may be considered as a combination of space charge limited, Schottky effect and Frenkel–Poole conduction. It was also found that, with increasing Gd content in PGZT $x/52/48$ ceramics, the current or loss tangent reduces significantly compared to PZT ceramics in such a way that the current first decreases for $x \leq 0.10$ and then increases for $x > 0.10$ in accordance with the variation of cell parameters in the studied ceramics [25].

4. Conclusion

The polycrystalline PGZT samples with Zr/Ti ratio = 52/48 (near MPB) and Gd content $x = 0, 0.07, 0.10$ and 0.12 were prepared by a high-temperature solid-state reaction technique which is cost-effective and less complex. In the present paper, we have reported the detailed analysis of electrical property such as conductivity and complex impedance-modulus analysis as a function of temperature and/or frequency and/or concentration of gadolinium. Complex impedance spectroscopy (CIS) analysis shows that the studied materials exhibit (i) the presence of bulk (grain) contributions which is found to decrease with the increase in temperature (NTCR behaviour), (ii) non-Debye-type conductivity relaxation, (iii) temperature and Gd-dependent relaxation and (iv) resistive property as a function of microstructure. Modulus spectrum analysis also suggests the non-Debye relaxation with gadolinium-dependant type relaxation in PGZT ceramics and the plateau region or its tendency observed at high frequencies indicates the frequency invariant-dependent electrical properties of the materials. The AC conductivity spectrum of PGZT electroceramics is found to obey Jonscher's universal power law and provides evidence of space charge accumulation in the material that vanishes at high frequencies and shows the possibility of hopping mechanism for electrical transport process. The nature of the $J-E$ curves shows that the conduction mechanism of PGZT ceramics is nonlinear, confirming the existence of non-Ohmic and space-charge limited conduction in the material. Hence, high resistivity and non-Ohmic behaviour of the studied materials are suitable for manufacturing high dielectric and non-linear ferroelectric ceramics.

References

- [1] M E Lines and A M Glass, *Principles and applications of ferroelectrics and related materials* (Oxford University Press, Oxford, 1977)
- [2] X Zhu, J Zhu, S Zhou, Z Liu and N Ming, *J. Am. Ceram. Soc.* **91**, 227 (2008)
- [3] G H Haertling, *J. Am. Ceram. Soc.* **82**, 797 (1999)
- [4] W Dong, L Xiaoguang, Y Cui, J Wang and M Liu, *Thin Solid Films* **515**, 8544 (2007)
- [5] D Ambica, V Kumar, K Tomioka and Isaku Kanno, *Adv. Mater. Lett.* **3**, 102 (2012)
- [6] M A Khan, T P Comyn and A J Bell, *J. Euro. Ceram. Soc.* **28**, 591 (2008)
- [7] C Guerrero, J Roldan, C Ferrater, M V Garcia-Cuenca, F Sanchez and M Varela, *Solid State Electron.* **45**, 1433 (2001)
- [8] S G Porter, *Mater. Des.* **8**, 120 (1978)
- [9] Rajiv Ranjan, Rajiv Kumar, Nawnit Kumar, Banarji Behera and R N P Choudhary, *J. Alloys Compd.* **509**, 6388 (2011)
- [10] K P Rema, Vinod K Etacheri and V Kumar, *Mater. Electron.* **21**, 1149 (2010)
- [11] R P Tondon, *J. Kor. Phys. Soc.* **32**, 327 (1998)
- [12] A K Sukla, V K Agrawal, I M L Das, Janardan Singh and S L Srivastava, *Bull. Mater. Sci.* **34**, 133 (2011)
- [13] J E Garcia, D A Ochoa, V Gomis, J A Eiras and R Perez, *J. Appl. Phys.* **112**, 014113 (2012)
- [14] K Ramam and M Lopez, *J. Alloys Compd.* **466**, 398 (2008)
- [15] W Qiu and H H Hng, *Mater. Chem. Phys.* **75**, 151 (2002)
- [16] S C Panigrahi, Piyush R Das, R Padhee and R N P Choudhary, *Ferroelectrics* **524**, 14 (2018)
- [17] S Singh, O P Thakur and Chandra Prakash, *Defence Sci. J.* **55**, 349 (2005)
- [18] Y Wang, X Hao, J Yang, J Xu and D Jhao, *J. Appl. Phys.* **112**, 034105 (2012)
- [19] D Kuscer, J Korzekwa, M Kosec and R Skulski, *J. Eur. Ceram. Soc.* **27**, 4499 (2007)
- [20] S Q Zhang, L D Wang, W L Li, N Li and W D Fei, *J. Alloys Compd.* **509**, 2976 (2011)
- [21] S K S Parasar, R N P Choudhary and B S Murty, *Mater. Sci. Eng. B* **110**, 58 (2004)
- [22] J Portelles, N S Almodovar, J Fuentes, O Raymond, J Heiras and J M Siqueiros, *J. Appl. Phys.* **104**, 073511 (2008)
- [23] S C Panigrahi, Piyush R Das, B N Parida, R Padhee and R N P Choudhary, *J. Alloys Compd.* **604**, 73 (2014)
- [24] S C Panigrahi, Piyush R Das, B N Parida, H B K Sharma and R N P Choudhary, *J. Mater. Sci: Mater. Electron.* **24**, 3275 (2013)
- [25] S C Panigrahi, Piyush R Das and R N P Choudhary, *Phase Transitions* **91**, 703 (2018)
- [26] J R Macdonald, *Impedance spectroscopy: Emphasizing solid state material and systems* (Wiley, New York, 1987)
- [27] R Chauhan and R C Srivastava, *Pramana – J. Phys.* **87**: 45 (2016)
- [28] P S Das, P K Chakrabarty, B Behera and R N P Choudhary, *Physica B* **395**, 98 (2007)
- [29] B N Parida, Piyush R Das, R Padhee and R N P Choudhary, *J. Phys. Chem. Solids* **73**, 713 (2012)
- [30] M Prabu, I B Shameem Banu, D Kannan, S Gobalakrishnan and Murthy Chavali, *J. Mater. Sci: Mater. Electron.* **24**, 1556 (2013)

- [31] J C Anderson, *Dielectrics* (Champan and Hall Ltd., London, 1963)
- [32] C K Suman, K Prasad and R N P Choudhary, *J. Mater. Sci.* **41**(2), 369 (2006)
- [33] F Borsa, D R Torgeson, S W Martin and H K Patel, *Phys. Rev. B* **46**, 795 (1992)
- [34] J R Macdonald, *Solid State Ion.* **13**, 147 (1984)
- [35] R Padhee, Piyush R Das, B N Parida and R N P Choudhary, *J. Mater. Sci: Mater. Electron.* **23**, 1688 (2012)
- [36] B Jaffe, W R Cook and H L Jaffe, *Piezoelectrics ceramics* (Academic Press, New York, 1971)
- [37] C G F Stenger and A J Burggraaf, *J. Phys. Chem. Solids* **41**, 25 (1980)
- [38] A K Jonscher, *Nature* **267**, 673 (1977)
- [39] K Funke, *Prog. Solid State Chem.* **22**, 111 (1993)
- [40] B Tiwari and R N P Choudhary, *J. Phys. Chem. Solids* **69**, 2852 (2008)
- [41] R Padhee, P R Das, B N Parida and R N P Choudhry, *Ferroelectrics* **437**, 160 (2012)
- [42] B Pati, R N P Choudhry and P R Das, *J. Alloys Compd.* **579**, 218 (2013)